JOURNAL OF Applied Polymer SCIENCE

Morphology and Properties of Poly(vinylidene fluoride)/Silicone Rubber Blends

Yanpeng Wang,[1,2] Liming Fang,[2] Chuanhui Xu,[1,2,3] Zhonghua Chen,[2] Yukun Chen[1,4]

[1]The Key Laboratory of Polymer Processing Engineering, Ministry of Education, China (South China University of Technology), Guangzhou 510640, China

[2]School of Materials Science and Engineering, South China University of Technology, Guangzhou 510640, China

[3]School of Chemistry and Chemical Engineering, Guangxi University, Nanning 530004, China

[4]School of Mechanical and Automotive Engineering, South China University of Technology, Guangzhou 510640, China

Correspondence to: Yukun Chen (E-mail: cyk@scut.edu.cn)

ABSTRACT: Blends of poly(vinylidene fluoride) (PVDF) and silicone rubber (SR) were prepared through melt mixing. The morphology, rheology, crystallization behavior, mechanical properties, dynamic mechanical properties and thermal properties of the PVDF/SR blends were investigated. The blend with 9 wt % of SR showed spherical shape of disperse phase whereas the blend with 27 wt % of SR resulted in irregular shape of rubber phase. The rheology showed that the complex viscosity and storage modulus of the blends decreased with increasing the SR content. The mechanical properties of the blends were decreased with increasing the SR content but that were significantly improved after dynamical vulcanization. The crystallization temperature of PVDF phase in PVDF/SR blends was increased. The incorporation of SR improved the thermal stability of PVDF/SR blends, and the temperature at 10% mass loss of the blends increased to about 489°C compared with 478°C of the pure PVDF. The mass of residual char in experiment of the blends was lower than that obtained in theory. © 2013 Wiley Periodicals, Inc. J. Appl. Polym. Sci. **2014**, *131*, 39945.

KEYWORDS: blends; morphology; rheology; thermogravimetric analysis

Received 22 April 2013; accepted 8 September 2013

DOI: 10.1002/app.39945

INTRODUCTION

In recent years, with the development of aerospace, military, automobile, and chemical industry, the requirements for the specialty elastomers in high and low temperature resistance, oil resistance, and chemistry resistance are increasing, whereas general rubber, such as nature rubber (NR), chloroprene rubber (CR), and nitrile rubber (NBR) etc., can not satisfy thermal stability, and oil resistance in new rubber productions. Fluororubber (FKM) has outstanding thermostability, oil and corrosion resistance, and silicone rubber (SR) exhibits high temperature stability, low temperature flexibility, and good processability, which lead to increase the application of FKM and SR. However, the disadvantages of FKM are lack of low temperature resistance and bad processability, and SR has a lack of oil resistance, thus fluorosilicone rubber with the advantages of FKM and SR gradually attracts people's attention, but fluorosilicone rubber cannot be widely used due to its high price and its complicated synthesis technology which is difficult to control.[1]

Preparation of polymer blends is an effective way to achieve the demand from parent polymer pairs. Blending of two polymers usually gives rise to a new material having a better balance of properties than obtainable with a single polymer. FKM/SR blends[1–4] are prepared by mechanical blending. The mechanical properties of FKM/SR blends are similar to those of fluorosilicone rubber but the preparation cost of FKM/SR blends is cheaper. As a result, FKM/SR blends can partially substitute important and expensive fluorosilicone rubber, but vulcanizaed FKM/SR blend is thermosetting material.

Fluoroplastic and FKM have partially similar physical properties. As one of the special functional fluroplastic, poly(vinylidene fluoride) (PVDF) has been widely studied owing to its remarkable mechanical properties, thermal stability, piezoelectric and pyroelectric properties, in combination with good resistance to high temperatures, UV irradiation, and aggressive chemicals.[5,6] Recently, many works reported in the literature are related to the blends of PVDF and various amorphous polymers, including poly (methyl methacrylate) (PMMA),[7] poly (vinyl fluoride) (PVF),[8] poly(vinylpyrrolidone) (PVP),[9] poly(3-hydroxybutyrate) (PHB)[10] and etc. During the last decades, many elastomers and thermoplastics were introduced to produce blends, such as NR/polystyrene (PS),[11] NR/polypropylene

Table I. Formulations of the Prepared Samples (Weight Ratio)

Coding	PVDF	SR	MgO	$Ca(OH)_2$	DCP
90/10	90	10	3	5	0
80/20	80	20	3	5	0
70/30	70	30	3	5	0
60/40	60	40	3	5	0
D60/40	60	40	3	5	0.8

(PP),[12] PP/NBR,[13] ethylene-propylene-diene terpolymer (EPDM)/PP,[14–17] and so on. However, little attention has been paid to the study on the PVDF/rubber blends.

Therefore, PVDF was chosen instead of FKM and the aim was to prepare a new thermoplastic elastomer based on PVDF and SR. Our laboratory has used dynamic vulcanization to prepare a new type of PVDF/SR blend.[18] The blends were prepared in the mixing chamber by dynamically curing dicumyl peroxide (DCP). Some special phenomenon might be observed for the first time. For example, the crosslinked spherical SR particles with an average diameter of 2–4 μm form a "network" in the PVDF continuous phase. The properties and morphology of the dynamically cured PVDF/SR blends have been investigated, but that of PVDF/SR blends without dynamically vulcanization is still unclear.

Thus, in this article, the PVDF-rich blends were studied. The morphology, mechanical properties, crystallization behavior, rheology, dynamic mechanical properties and thermal properties of the blends were investigated as a function of the PVDF/SR blend composition.

EXPERIMETAL

Materials

Poly(vinylidene fluoride) (PVDF 502) was purchased from Guangzhou Li Chang Fluoroplastics. SR was a commercial rubber (KE 571-U, Shin-Etsu, Japan). Magnesium oxide (MgO) and Calcium hydroxide ($Ca(OH)_2$) were purchased from Shanghai TongYa Chemical Technology (China). DCP was purchased from Sinopharm Chemical Reagent (Shanghai, China) and was purified by anhydrous alcohol recrystallization before use.

Compositions and Sample Preparation

PVDF/SR blends with weight ratios of 90/10, 80/20, 70/30, and 60/40 were prepared by melt mixing using an internal mixer (Haake Rheocord 90, Germany), which were denoted as 90/10, 80/20, 70/30, and 60/40, respectively. $MgO/Ca(OH)_2$ were used as stabilizing agents. To investigate the effect of dynamical vulcanization, one sample based on the PVDF/SR blend with weight ratio of 60/40 was also prepared which was denoted as D60/40. The concentrations ratio between SR and DCP was maintained as constant (SR/DCP = 100/2). The compositions in terms of the weight ratios of components for PVDF/SR blends are presented in Table I.

The mixer temperature and rotor speed were kept at 190°C and 90 rpm, respectively. PVDF was first incorporated into the internal mixer for about 4 min, followed by the addition of SR, the mixing was continued until a final stable torque was reached. The total mixing process lasted about 8 min. Subsequently, the blends were removed from the internal mixer and cooled at room temperature before being granulated. For D60/40, DCP was added at around 7 min. All the specimens for mechanical testing were prepared by injection molding (TTI-160F, Welltec Machinery & Equipment, China). The nozzle temperature was 220°C, and the injection pressure was 50 MPa.

Mechanical Properties Measurements

Standard tensile tests were conducted on dumbbell shaped specimens using a universal testing instrument (Shimadzu AG-1, 10 kN, Japan) with a tensile mode at room temperature. Test speed was kept at 50 mm/min, according to GB/T 1040-2006 standard. The flexural strength was also measured using universal testing instrument (Shimadzu AG-1, 10 kN, Japan), at a speed of 20 mm/min according to GB 9341-2008 standard. The notched Izod impact strength was used to evaluate the toughness of the samples. The notched specimens were tested with an impact test machine (ZWICK5331, Germany, Zwick/Roell) at room temperature, according to GB/T 1843-2008 standard. All the above tests were repeated at least five times, and the results were averaged.

Morphological Studies

Nova Nano SEM 430 (FEI Company) was used to investigate the phase morphology of the blends. Before morphological observation, the surface of samples was coated with a thin layer of gold to prevent electrostatic charging build-up during observation.

Rheological Characterization

Melt rheological behaviors of the blends were analyzed by using a Rubber Process Analyzer (RPA 2000, Alpha Technologies) equipped with bi-conical test fixtures. Samples were approximately about 6 g and were placed between two polyester films. The melted test specimens were directly loaded between the dies at 210°C and the tests were carried out in both strain sweep and frequency sweep modes. Strain amplitude sweep was performed from 1 to 70% at a constant frequency of 1 Hz. Frequency sweep was performed at frequencies ranging from 0.33 to 33 Hz at constant strain amplitude of 5%.

Dynamic Mechanical Analysis

The dynamic mechanical behavior of the peroxide dynamical vulcanized blends was determined by using a dynamic mechanical analyzer (DMA242C NETZSCH; Germany) with three-point bending mode at 10 Hz with a heating rate of 5°C/min from −150 to 80°C. The samples were prepared as a cut strip with the size of 30 mm × 6 mm × 4 mm.

Differential Scanning Calorimetry Analysis

Melting and crystallization behavior of the blends were measured in nitrogen atmosphere using a differential scanning calorimeter (DSC 204F1 NETZSCH, German). For each test, a 5–6 mg sample was first heated to 220°C at a rate of 10°C/min and was then kept at this temperature for 5 min to eliminate previous thermal history. Then the sample was cooled to room temperature at a cooling rate of 20°C/min and then secondly heated to 220°C at a heating rate of 10°C/min for data collection.

Thermal Gravimetric Analysis

A thermogravimeter (TGA 209, NETZSCH, Germany) was used to measure the weight loss of the dynamically vulcanized

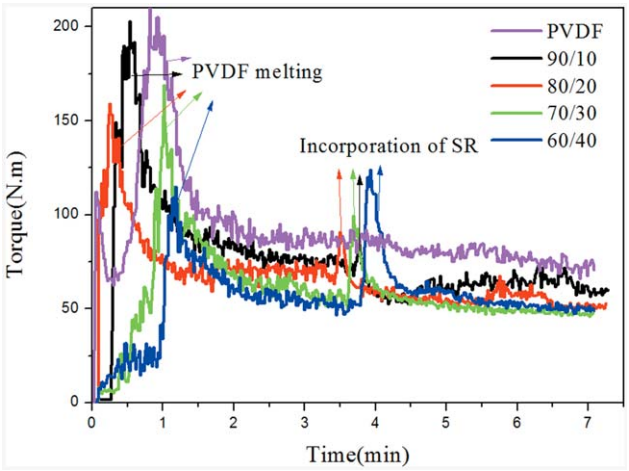

Figure 1. Plot of torque versus time for the PVDF/SR blends at 190°C. [Color figure can be viewed in the online issue, which is available at wileyonlinelibrary.com.]

PVDF/NBR blends under nitrogen atmosphere. The samples were heated from ambient temperature up to 900°C at a heating rate of 20°C/min. Generally, approximately 10 mg of samples were used for each thermogravimetric analysis.

RESULTS AND DISCUSSION

The Torque of Mixing

Figure 1 shows the torque change during preparing PVDF/SR blends at 190°C. The first peak was related to the PVDF melting. After the PVDF completely melted, it was observed that the torque value reduced with the PVDF content decreased. The second peak corresponded to the incorporation of SR. The SR component seemed to lower the final torque value of the blends, which might be attributed to the low viscosity of SR and the poor compatibility between the PVDF and SR phase. The final torque value for the 80/20 showed a small decrease compared with the 90/10. For the 70/30 and 60/40, the torque values were similar, which indicated the SR phase had a little influence on the viscosity of the blends when the PVDF/SR ratio exceeded 70/30.

Mechanical Properties

The mechanical properties of the PVDF/SR blends are presented in Table II. The tensile strength, flexural strength, flexural modulus, and Izod impact strength of the neat PVDF were 54.0 MPa, 68.8 MPa, 1602 MPa, and 12.4 kJ/m^2, respectively. Incorporation of 9 wt % of SR decreased tensile strength, flexural strength, flexural modulus by 25%, 21% and 9%, respectively. Further increasing SR content led to a regular drop in tensile strength, flexural strength and flexural modulus. At 37 wt % SR content, tensile strength, flexural strength, flexural modulus of the blend was 9.3 MPa, 10.6 MPa, 243 MPa, decreased higher by 83%, 85% and 85%, respectively. The reduction of PVDF matrix and poor compatibility between the PVDF and SR phase should be responsible to the decreased mechanical properties. The poor compatibility between the two components also could be deduced from the decreased Izod impact strength of the blends. The mechanical properties of the blends was decreased due to the incorporation of SR. Compared 60/40 with D60/40, it was found that the tensile strength, flexural strength, flexural modulus of D60/40 was 15.1 MPa, 17.9 MPa, and 432 MPa, respectively, which was increased by 62.4%, 68.9%, and 77.8%, indicating that the dynamical vulcanization significantly improved the mechanical properties of blends, however, the Izod impact strength of D60/40 was lower than that of 60/40. According to the literature,[2] the tensile strength of FKM/SR (weight ratio = 75/25) blend was 7.8 MPa, that of PVDF/SR (60/40) blend was 9.3 MPa lowest in the system, but still higher than that of the FKM/SR (weight ratio = 75/25) blend. Therefore the fluoroplastic/SR blend could partially substitute FKM/SR blends in some areas.

Morphology of the PVDF/SR Blends

As shown in Figure 2, the surface of 90/10 was rugged but relative "flat". With the SR content increased, the surface of 70/30 appeared some irregular "gap" which might be due to the SR dropped off the matrix.

The sample was extracted by hot tetrahydrofuran wash to remove the rubber phase at the surface layer. As shown in Figure 3, many "holes" represented as the SR phase were observed. In the case of the 90/10 blend [Figure 3(a)], it can be seen that the SR spherical particles with the diameter of 1–3 μm were distributed in the continuous PVDF matrix. For the 70/30 blend, the irregular shapes of rubber particles including spherical and elliptical shapes were observed. The maximal and minimum diameter of the "holes" was 8 μm and 0.5 μm, respectively. The interface and margin of the "holes" was quite smooth and bright, which indicated a weak interaction between the PVDF continuous phase and the SR dispersed phase, leading to the decrease of the impact strength. This is also in accordance with the mechanical properties discussed above.

Rheology

The strain sweep experiment carried out at 210°C shows the effect of shear strain on the storage modulus (G') and complex viscosity (η^*) (Figure 4). The elastic behavior of an immiscible polymer blend system can be investigated by measuring the storage modulus of the system under isothermal condition at

Table II. Mechanical Properties of the PVDF/SR Blends

	PVDF	90/10	80/20	70/30	60/40	D60/40
Tensile strength (MPa)	54.0	40.5	27.7	17.8	9.3	15.1
Flexural strength (MPa)	68.8	54.4	36.2	20.8	10.6	17.9
Flexural modulus (MPa)	1602	1462	1065	596	243	432
Izod impact strength (kJ/m^2)	12.4	8.9	8.5	7.7	7.1	5.5

Table III. Temperature for Tan δ_{max} of the PVDF/SR Blends

	PVDF phase	SR phase
PVDF	−28.4	-
90/10	−25.1	−102.6
80/20	−23.3	−101.8
70/30	−22.0	−104.4
60/40	−20.8	−103.4

small amplitude of oscillatory shear flow. It can be also seen that the storage modulus of the pure PVDF was almost kept constant, but that of the blends decreased with increasing strain amplitude [Figure 4(a)]. The storage modulus showed a significant decrease as the rubber content increased in the blends and this had been attributed to the effect of the poor interfacial adhesion between the PVDF and SR phase.

The strain dependence of the complex viscosity (η^*) for the blends is shown in Figure 4(b). The viscosity decreased with increasing strain which implied pseudoplastic behavior. The η^* curves were similar to the G' curves. The complex viscosity of the pure PVDF showed no significant change and the value was kept at about 3700 Pa s. When the shear stress was applied at a high temperature, the polymer blends underwent deformation and elongational flow. When the interfacial interaction was strong, the deformation of the dispersed phase would be effectively transferred to a continuous phase. However, in the case of weak interfacial interaction, inter layer slip occurred, as a result, the viscosity of the system decreased. This can be confirmed that the interfacial interaction between the PVDF and SR was weak, which was in accordance with the mechanical properties discussed above. It was important to note that the viscosity decreased with the rubber content increased. But according to the previous literature,[19] the viscosity increased with the rubber content increased, and for the dynamical cured PVDF/SR blends system,[18] the complex viscosity of the blends also increased as the rubber content increased. This special phenomenon in this system might be attributed to the nature characterization of the SR. Because the SR was uncured, the interfacial interaction with uncrosslinked SR was weaker and the SR phase with low viscosity distributed in the PVDF matrix, which might play the dilution effect and lubrication action, and then leaded to the viscosity of the blends decreased, which was also in accordance with the final torque values obtained from the Figure 1.

Figure 5 shows the logarithmic plot of dependence of complex modulus (G^*) and complex viscosity (η^*) as a function of frequency for the blends with different PVDF/SR ratios. The G^* increased with the frequency increased, but η^* decreased as the frequency increased. The SR content had a little influence on the complex modulus and complex viscosity, especially at high frequency. It was different when the SR phase was cured, which was attributed to the weak interfacial interaction between PVDF phase and SR phase when the SR phase was uncured.

Dynamic Mechanical Properties Analysis

Dynamic mechanical properties are widely used to investigate phase evolution in immiscible blends thanks to their sensitivity to phase change. Figure 6 shows the temperature dependence of storage modulus (E') and tan δ of PVDF/SR blends with different compositions. The E' and G' [Figure 4(b)] showed the similar trend that the E' of the PVDF/NBR blends was decreased as increasing SR content, since the decreased PVDF continuous phase in the blends. Two distinct peaks of tan δ each corresponding to the glass transition temperatures of PVDF and SR can be observed in all the blends, indicating the immiscibility between the two phases. The one at around −24°C was related to the glass-rubber transition of the PVDF phase and the other at around −100°C corresponded to the glass-rubber transition of the SR phase (Table III). The T_g of the pure PVDF was −28.4°C. Interesting, T_g of the PVDF phase was shifted to higher temperature from −25.1 to −20.8°C as increasing the SR content. In fact, MgO and $Ca(OH)_2$ may not be averagely distributed in the blends. Perhaps, with increasing SR content, MgO and $Ca(OH)_2$ in PVDF phase relatively increased and resulted in the experimental results.

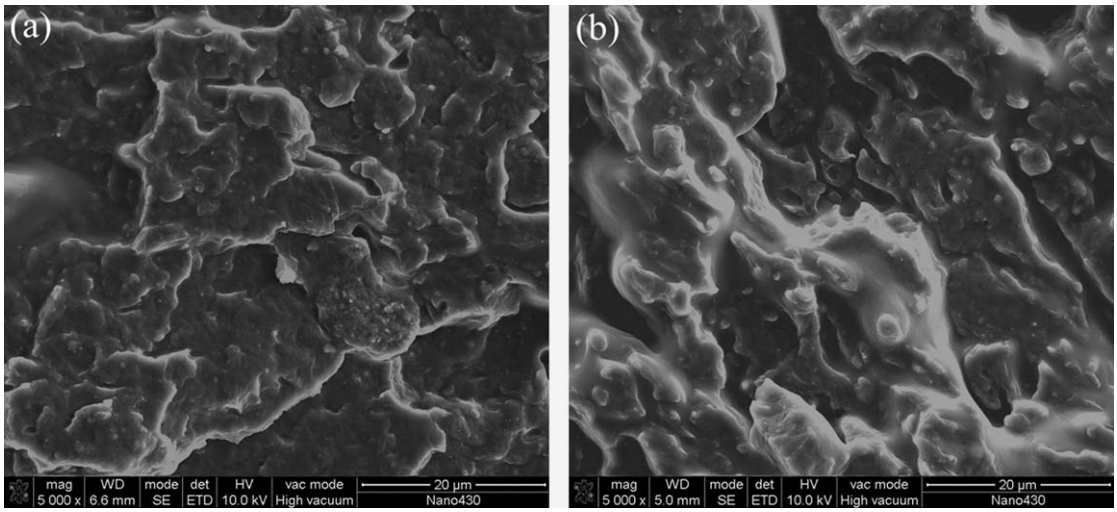

Figure 2. SEM micrograph of cryogenically fractured surface of 90/10 and 70/30 blends.

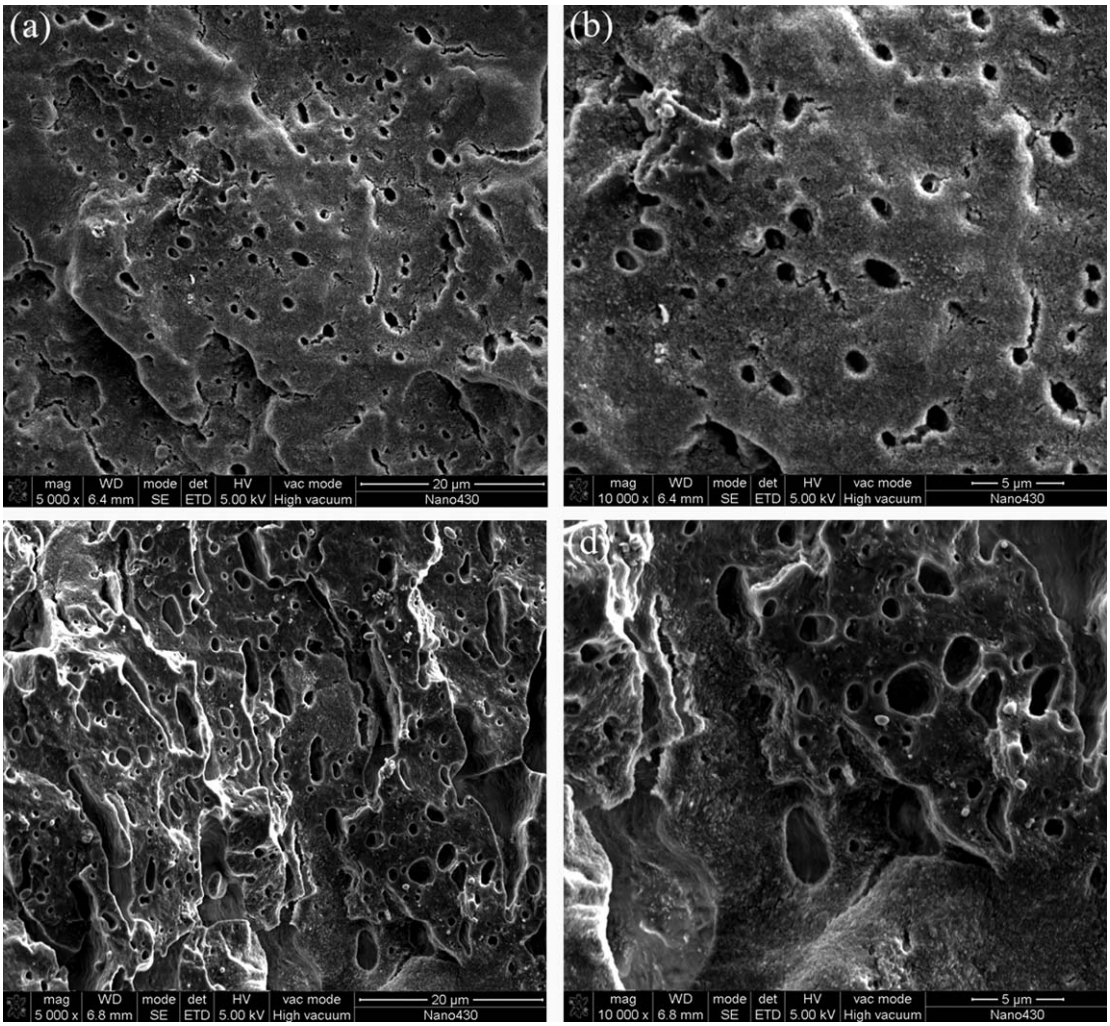

Figure 3. Cryogenically fractured surface etched by tetrahydrofuran: (a) 90/10 (×5000); (b) 90/10 (×10,000); (c) 70/30 (×5000); and (d) 70/30 (×10,000).

Crystallization Behavior

Figure 7 shows the melting curves and crystallization curves of the blends. The effects of SR on the crystallization peak temperature (T_c), the melting temperature (T_m), and the onset of crystallization temperature (T_o) are summarized in Table IV. It is clearly seen that the T_m of the PVDF phase in the blends was slightly

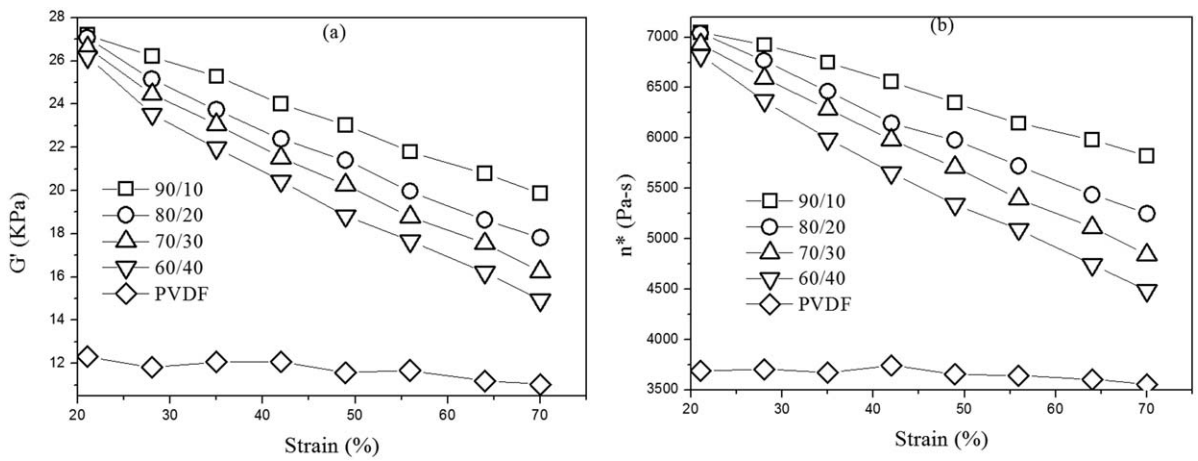

Figure 4. Melt rheological properties as a function of strain at 210°C: (a) Storage modulus, (b) Complex viscosity.

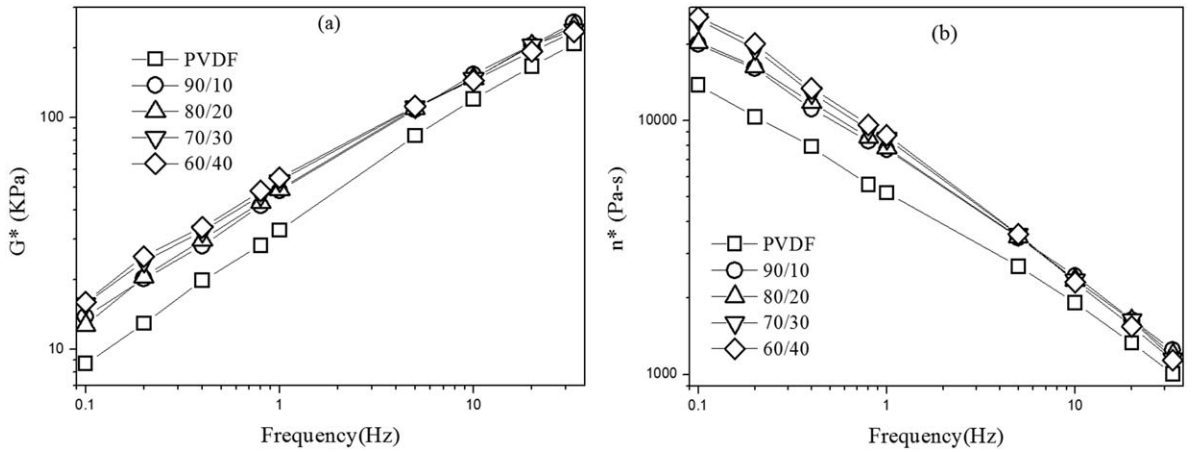

Figure 5. Complex modulus (a) and complex viscosity (b) as a function of frequency.

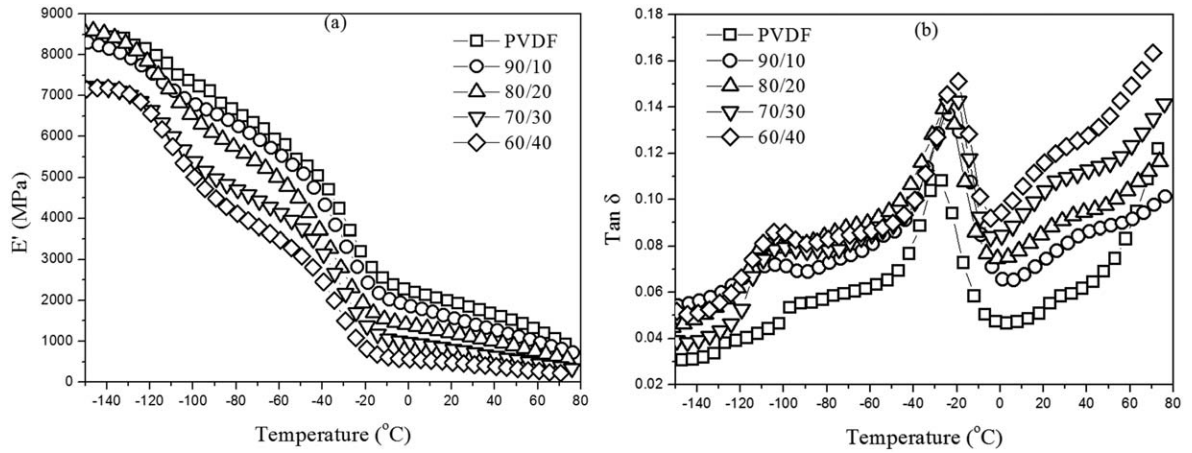

Figure 6. Storage modulus E' (a) and loss factor tan δ (b) versus temperature at 10 Hz.

lower than that of the pure PVDF, whereas the T_c and T_o of the blends are higher than that of the pure PVDF, suggesting that the incorporation of SR promoted the crystallization process of the PVDF phase, accelerating the crystallization of PVDF in the blends and increasing the crystallization temperature.

Thermal Properties of PVDF/SR Blends

The thermal stability of the PVDF/NBR blends was evaluated through the weight loss in nitrogen using thermal gravimetric analysis (TGA), and the values of weight loss at different temperatures are summarized in Table V.

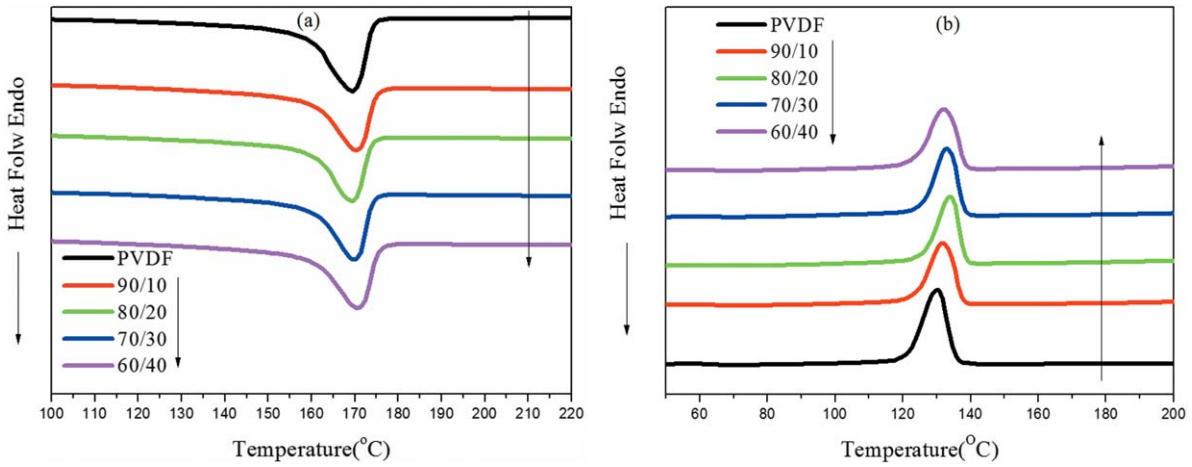

Figure 7. DSC curves of the blends: (a) melting curves, (b) crystallization curves. [Color figure can be viewed in the online issue, which is available at wileyonlinelibrary.com.]

Table IV. Crystallization Parameters of the PVDF and the Blends

	PVDF	90/10	80/20	70/30	60/40
T_m (°C)	171.5	170.2	169.4	169.9	170.7
T_c (°C)	130.1	131.8	134.0	133.0	132.0
T_o (°C)	135.5	137.7	138.4	138.2	138.5

As shown in Figure 8, the thermogram of pure PVDF and SR showed the typical single degradation step profile. As shown in Table IV, the thermogram of pure PVDF and SR showed the typical single degradation step profile. The main PVDF degradation occurred between 450°C and 500°C, and the main SR degradation occurred between 500°C and 650°C, indicating that both the PVDF and SR have the excellent thermal stability. The incorporation of SR component obviously increased the onset decomposition temperature of the PVDF phase. The temperature corresponding to 10% weight loss for the neat PVDF was 478°C, whereas this temperature became 489°C in the presence of 9 wt % SR. When the SR content was increased to 37%, the temperatures at 10% weight loss increased to 490°C. Similarly, at 50% weight loss, the temperatures corresponding to the PVDF and SR were 497°C and 597°C, respectively. The SR content had no obvious influence on temperatures at weight loss of the blends, the temperature at 10%, 30%, 50% weight loss of the blends was about 489°C, 500°C and 505°C, respectively. The mass of residual char in experiment of PVDF and SR was about 15% and 38%, respectively. Mass of residual char in theory (M_t) of the blends can be calculated according to the following equation:

$$M_t = \frac{0.15X + 0.38Y + Z}{T} \times 100\% \quad (1)$$

where X, Y, Z, and T represents weight of PVDF, SR, stabilizing agents and total weight of the blend, respectively. The mass of residual char in experiment of the blends increased with the content of SR increased which was higher than that of the neat PVDF. Interestingly, the mass of residual char in theory was higher than that obtained from experiment. Seen from Figure 7(b), the temperature of maximum thermal decomposition of the neat PVDF and SR was 495°C and 605°C, and the temperature of maximum thermal decomposition of the blends was higher than that of the neat PVDF, indicating that the incorporation of SR component improved the thermal stability of PVDF/SR blends to a certain extent. But the blends indicated single peak, which was closed to the thermal decomposition peak of the PVDF. The thermal decomposition peak of the SR in the blends was disappeared. It was thought that a series of complicated chemical reaction possible occurred simultaneously during heating, such as:

$$\mathrm{PVDF} \xrightarrow{\Delta} \mathrm{HF} \quad (2)$$

Table V. TGA Parameters for the PVDF/SR Blends

	Temperatures at 10% weight loss (°C)	Temperatures at 30% weight loss (°C)	Temperatures at 50% weight loss (°C)	Mass of residual char in experiment (%)	Mass of residual char in theory (%)
PVDF	478	490	497	15	15
90/10	489	500	505	20	23
80/20	488	499	507	21	26
70/30	489	499	504	22	28
60/40	490	500	505	26	30
SR	517	586	643	38	38

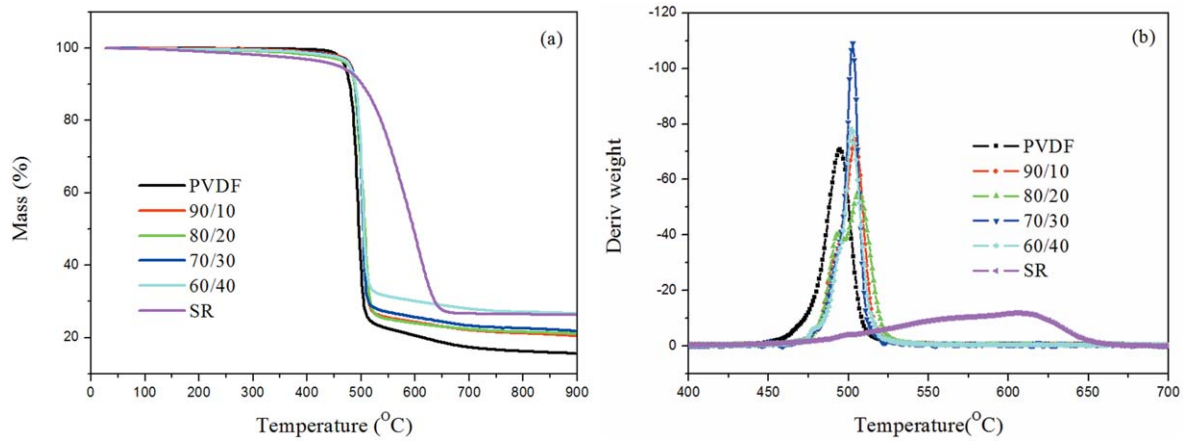

Figure 8. TGA (a) and DTG (b) curves of the PVDF/SR blends. [Color figure can be viewed in the online issue, which is available at wileyonlinelibrary.com.]

$$SR \xrightarrow{\Delta} SiO_2 \quad (3)$$

$$4HF + SiO_2 \xrightarrow{\Delta} SiF_4 \uparrow + 2H_2O \quad (4)$$

Here, eq. (2) represented the PVDF during thermal decomposition generated hydrogen fluoride and eq. (3) represented the degradation of SR chains and generated silicon dioxide, eq. (4) represented the reaction between hydrogen fluoride and silicon dioxide, the hydrogen fluoride and silicon dioxide were consumed and the gas (SiF_4) was generated finally. Thus the mass of residual char of the blends should be lower than that obtained in theory. Seen from Table IV, the mass of residual char in experiment for 90/10 was 20%, but that in theory was 23%. The mass of residual char in experiment for 60/40 was 26%, but the value obtained in theory was 30%. This proved that the chemical reaction discussed above possibly occurred.

CONCLUSIONS

PVDF/SR blends with different compositions were prepared through melt mixing process. Morphology characterization showed that the PVDF/SR blend was an incompatible system. Although the mechanical properties of the blends were decreased with the SR content increased, the dynamical vulcanization significantly improved the mechanical properties. The blend with 9 wt % of SR showed spherical shape of disperse phase whereas the blend with 27 wt % of SR resulted in irregular shape of rubber phase. The rheology study showed that with the increase of the rubber content, the blends retained pseudoplastic nature, but the complex viscosity and storage modulus of the blends decreased with increasing the SR content which was attributed to the nature characterization of SR. The incorporation of SR component promoted the crystallization process of PVDF, leading to increase the crystallization temperature. The incorporation of SR improved the thermal stability of PVDF/SR blends, and the temperature at 10% mass loss of the blends increased to about 489°C compared with 478°C of the pure PVDF. The mass of residual char in experiment of the blends was lower than that obtained in theory.

ACKNOWLEDGMENTS

This work was financially supported by the Fundamental Research Funds for the Central Universities (2012ZZ0018).

REFERENCES

1. Guo, J. H.; Zeng, X. R.; Luo, Q. K. *J. Elastom. Plast.* **2009**, *41*, 554.
2. Ghosh, A.; Kumar, B.; Bhattacharya, A. K.; De, S. K. *J. Appl. Polym. Sci.* **2003**, *88*, 2377.
3. Kim, D. H.; Hwang, S. H.; Kim, B. S. *J. Appl. Polym. Sci.* **2012**, *125*, 1625.
4. Kim, D. H.; Hwang, S. H.; Park, T. S.; Kim, B. S. *J. Appl. Polym. Sci.* **2013**, *127*, 561.
5. Kawai, H. *Jpn. J. Appl. Phys.* **1969**, *8*, 975.
6. Lovinger, A. J. *Science* **1983**, *220*, 1115.
7. Okabe, Y.; Murakami, H.; Osaka, N.; Satio, H.; Inoue, T. *Polymer* **2010**, *51*, 1494.
8. Gupta, A. K.; Bajpai, R.; Keller, J. M. *J. Mater. Sci.* **2006**, *41*, 5857.
9. Chen, N. P.; Hong, L. *Polymer* **2002**, *43*, 1429.
10. Liu, J. P.; Jungnickel, B. J. *J. Polym. Sci. Part B: Polym. Phys.* **2003**, *41*, 873.
11. Asaletha, R.; Kumarana, M. G.; Thomas, S. *Eur. Polym. J.* **1999**, *35*, 253.
12. Ismail, H.; *Suryadiansyah Polym. Test.* **2002**, *21*, 389.
13. Xu, C. H.; Cao, X. D.; Jiang, X. J.; Zeng, X. R.; Chen. Y. K. *Polym. Test.* **2013**, *32*, 507.
14. Jiang, W.; Tjong, S. C.; Li, R. K. Y. *Polymer* **2000**, *41*, 3479.
15. Chen, Y. K.; Xu, C. H.; Cao, L. M.; Cao, X. D. *Mater. Chem. Phys.* **2013**, *138*, 63.
16. Martin, G.; Barres, C.; Sonntag, P.; Garois, N.; Cassagnau, P. *Mater. Chem. Phys.* **2009**, *113*, 889.
17. Chen, Y.K.; Xu, C. H.; Cao, L. M.; Wang, Y. P.; Fang, L. M. *J. Phys. Chem. B* **2013**, *117*, 7819.
18. Wang, Y. P.; Fang, L. M.; Xu, C. H.; Chen, Z. H.; Chen, Y. K. *Polym. Test.* **2013**, *32*, 1072.
19. Jose, J.; Nag, A.; Nando, G. B. *J. Polym. Environ.* **2010**, *18*, 155.